Journal of Oceanology and Limnology
Vol. 36 No. 5, P. 1527-1536, 2018
https://doi.org/10.1007/s00343-019-7278-y

Upper-ocean temperature trends in the Eastern China Seas during 1976–1996*

WANG Yuqi (王玉琦), LIN Xiaopei (林霄沛)**, LI Ziguang (李子光)

Physical Oceanography Laboratory/CIMST, Ocean University of China and Qingdao National Laboratory for Marine Science and Technology, Qingdao 266100, China

Received Oct. 11, 2017; accepted in principle Nov. 6, 2017; accepted for publication Nov. 10, 2017

Abstract Temperature in the Eastern China Seas (ECS), including the Bohai, Yellow, and East China seas, is crucially important with regard to weather forecasting and fishery activities of adjacent countries. Although sea surface temperature (SST) in the ECS has demonstrated a dramatically accelerated trend of warming after a regime shift (1976–1996), trends beneath the surface remain poorly understood because of the sparsity of observations. This study used in situ hydrographic data from 1976 to 1996 to examine upper-ocean temperature trends in the ECS. It was found that the multilevel trends show consistency with that of the surface water; i.e., warming is faster in winter than summer. However, the magnitudes of the trends weaken with increasing depth. Furthermore, the seasonal difference in the upper ocean is mainly associated with the warm currents in the ECS, which implies an essential contribution from horizontal advection. These phenomena could also be detected from data acquired from the routinely observed PN and 34°N sections. The spatiotemporal patterns of temperature trends in the upper ECS extend our understanding beyond the SST, especially highlighting the role of ocean dynamics in forming temperature patterns beneath the surface in comparison with atmospheric effects.

Keyword: upper ocean; temperature trends; Eastern China Seas

1 INTRODUCTION

The Eastern China Seas (ECS), including the Bohai, Yellow, and East China seas, are marginal seas that interact with the western Pacific Ocean. The spatiotemporal variations of temperature in the upper-ocean layer of the ECS play an important role in the coastal climate and ecological environment, especially with regard to fishery and weather forecasting activities of surrounding countries (Lin et al., 2001, 2005; Cai et al., 2006). Previous studies have detected a significant trend of sea surface temperature (SST) warming in the ECS during the past several decades (Lin et al., 2001; Chen and Ho, 2002; Wu et al., 2005; Zhang et al., 2005). This warming has been attributed to many intricate factors, such as the monsoon, oceanic advection, vertical mixing, and bathymetry (Xie et al., 2002; Liu et al., 2005; Feng and Lin, 2009; Tang et al., 2009; Zhang et al., 2010; Liu and Zhang, 2013). However, because of the lack of adequate observations throughout the ECS, the warming patterns cannot be identified clearly and debate continues regarding their controlling mechanisms.

Using reconstructed SST data and reanalysis products, attempts have been made to elucidate the mechanism behind the enhanced warming in the ECS. Based on century-long oceanic and atmospheric reanalysis products, a “hot spot” phenomenon has been identified (Wu et al., 2012); i.e., the trend of SST warming in the region of the western boundary currents is two to three times faster than the global mean. It has been suggested that this enhanced warming is associated with intensification of subtropical western boundary currents, although there is no observational evidence to verify this. Similarly, using reconstructed SST products, significant SST

* Supported by the China’s National Key Research and Development Projects (No. 2016YFA0601803), the National Natural Science Foundation of China (Nos. 41490641, 41521091, U1606402), and the Qingdao National Laboratory for Marine Science and Technology (No. 2015ASKJ01)
**Corresponding author: linxiaop@ouc.edu.cn

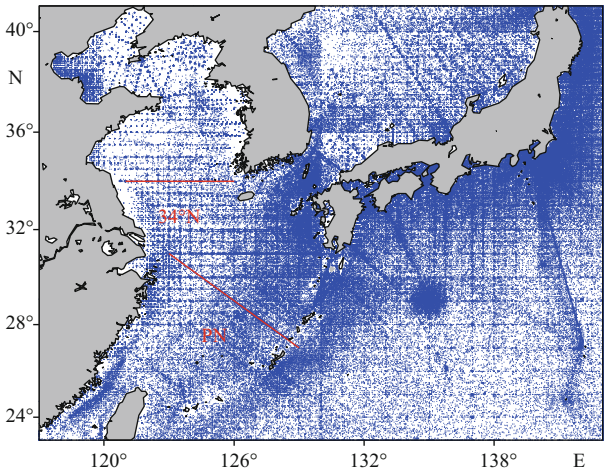

Fig.1 Spatial distribution of observational temperature data in the ECS

Blue dots denote in situ observations and the routine sections (34°N and PN) are depicted by red bold lines.

warming has been detected for the period 1945–2006 (Feng and Lin, 2009), highlighting the leading contribution from oceanic advection, despite the damping effect from surface heat flux. Progress on this topic could be advanced through the accumulation of samples both on spatial and on temporal scales. Using historical data, Wang et al. (2013) identified robust warming trends and complex spatial structures of SST in the ECS and they attributed the winter warming to horizontal advection. Earlier, using the same database, Tang et al. (2009) had considered the atmospheric contribution to winter warming after 1976, which produced results that were not confirmed by the later study.

Variations in upper-ocean temperature have been investigated widely in many previous works (Levitus et al., 1994; Smith, 1995; White, 1995), and it has been suggested that subsurface ocean dynamics are important for low-frequency SST variations in the open ocean (Latif and Barnett, 1994; Tomita et al., 2002). The prominent “hot spot” lies along the major path of the Kuroshio Current in the ECS region, where subsurface observations are of crucial importance but accessibility is difficult. Given the insufficient quantity of long-term observations in the ECS, reconstructed datasets and reanalysis products might have biases in capturing the changes of oceanic processes, resulting in inaccurate conclusions (Zhang et al., 2010). Furthermore, although satellite-derived products can provide accurate SST observations with high resolution both temporally and spatially, they are restricted to the surface and they do not provide adequate cover of the period of rapid warming after the regime shift (1976–1996). In addition, analyses based on surface observations have been unable to produce consensus on the mechanisms of warming in the ECS because of the neglect of the role of subsurface oceanic processes.

This study collected in situ hydrographic data from the ECS (Fig.1) that were obtained during large-scale marine hydrological surveys undertaken by many research institutes both in China and in adjacent countries. We constructed the spatial patterns of the linear trends of annual mean and seasonal upper-ocean temperature during the period of rapid warming period (1976–1996). Our analysis was not limited to the surface but it also considered several representative layers below the surface. Furthermore, temperature variations detected on routine sections along the paths of major warm currents were examined to assess the role of horizontal advection in the warming trends. To verify our results, the upper-ocean temperature of the latest Ishii dataset was also investigated, which realized consistent conclusions. Our results reveal the relative contributions of oceanic and atmospheric dynamics in forming the seasonal differences in the patterns of SST trend.

The remainder of this paper is organized as follows. Descriptions of both the data and the methods used are given in Section 2. Section 3 presents the results based on the hydrographic observational data, depicting the spatial patterns of the trends derived from the annual and the seasonal mean upper-layer temperatures in the ECS. Then, the temperature trends on two long-standing routine sections (PN and 34°N) are investigated. Finally, a brief discussion and our conclusions are presented in Section 4.

2 DATA AND METHOD

2.1 Data

Historical temperature data used in this study were derived mainly from the Ocean Science Database of the Institute of Oceanology, Chinese Academy of Sciences, with supplementary observations from other Chinese research institutes. This database has been compiled from data obtained during various Chinese investigations and from shared international datasets including the World Ocean Database 2001 of the National Ocean Data Center (Levitus et al., 2002). The primary quality control followed the methods reported by Boyer and Levitus et al. (2002). The data comprised 963 635 profiles obtained during 1976–1996, including temperature and salinity data at standard depths (0, 5, 10, 20, 30, 50, 75, 100, 125, and

150 m) and at the bottom. The spatial distribution of the temperature data and the extent of the study area (23.5°–41.5°N, 117.5°–143.5°E) are presented in Fig.1. According to preliminary statistics, the data coverage was sparse before the 1970s but comparatively denser after the 1970s.

For validation and supplementary support, we also used objectively analyzed monthly data (1945–2003) prepared by Ishii et al. (2003, 2006) covering subsurface temperature and salinity at 24 levels in the upper 1 500 m. The analysis was based on the World Ocean Database and Atlas (ds285.0), global temperature-salinity in the tropical Pacific Ocean from L'Institut de Recherche pour le Développement (France, ds279.1), and Centennial in situ Observation-Based Estimates of SST.

2.2 Data processing

To reduce bias caused by cruise-dependent spatial resolution and maximum observation depth, grid-consistent temperature fields were reconstructed using the Cressman (1959) interpolation. Restricted by bathymetry and inadequate sampling in deeper layers, the observed temperature was gridded to render spatial resolution of 1°×1° for the monthly time series at standard depths from the surface to 100 m (all layers not shown). This inferred the temperature $\phi_{i,j}$ at grid point (i, j) based on the surrounding observed temperature ϕ^k_{obs} at point k as

$$\phi_{i,j}=\sum_{k=1}^{N} W_{i,j}\varphi^k_{\text{obs}}, \tag{1}$$

where N is the total number of observed data, $W_{i,j}$ is the weight for the gridded data at (i, j) and observed data at k, which is generally calculated using the Cressman (1959) method. Weight $W_{i,j}$ is expressed as

$$W_{i,j}=\frac{W^k_{i,j}}{\sum_{k=1}^{N} W^k_{i,j}}, \tag{2}$$

where

$$W^k_{i,j}=\frac{R^2-r^2_{i,j}}{R^2+r^2_{i,j}}, \text{ for } r_{i,j}<R, \tag{3}$$

and

$$W^k_{i,j}=0, \text{ for } r_{i,j}\geq R, \tag{4}$$

where $r_{i,j}$ is the spatial distance between grid point (i, j) and observation point k, and R is the search radius, which was set at 1° in this study.

The relation that exists between temperature x_i and time y_i can be described using unary linear regression and reconstructing the time series of the estimator y_i* that satisfies the following formula:

$$y_i^*=y_0+kx_i, \tag{5}$$

where k and y_0 can be computed using the least squares approach, and where slope k represents the linear trend of the time series.

It is believed that an abrupt regime shift after 1976 accelerated the warming trends of sea temperature in the ECS (Tian et al., 2003; Cai et al., 2006), although a warming hiatus has been detected during 1998–2012 (Easterling and Wehner, 2009; Chen et al., 2014; Lin et al., 2016). This study focused on the variations of sea temperature during the period of rapid warming (1976–1996) when observational coverage was considered reasonable. Furthermore, temperature trends of the routine sections (PN and 34°N) were obtained from interpolated field observational data, following methods for data gridding similar to Wei et al. (2013), as well as from analysis of the Ishii dataset. We calculate the linear trends on the PN section for the area 31°–27°N, 123°–129°E. The vertical structure of temperature variation on the 34°N section extended from 121° to 126°E (Fig.1, red bold line).

3 RESULT

3.1 Area-averaged temperature trends

Using monthly upper-ocean observations, we constructed time series of annual mean temperature anomalies for the entire ECS at each representative layer, which were then separated into summer and winter seasons (Fig.2). For SST (0 m), the annual mean shows a significant warming trend, which can also be identified in winter and summer. The subsurface trends display consistency with the surface, although the magnitude of the warming decreases with increasing depth. For example, the annual mean trend is 0.06°C/a at the surface, which decreases gradually to 0.01°C/a at the depth of 100 m (Fig.2a). Furthermore, the trends show obvious seasonal difference; i.e., the rate of warming in winter is two to three times greater than in summer from the surface to 100 m. For example, values of 0.09 and 0.03°C/a at the surface weaken to about 0.03 and 0.01°C/a at 100 m in winter and summer, respectively (Fig.2b, c). In addition, plots of the regional mean time series indicate interannual variations during 1976–1996, as reported in earlier studies (Park and Oh, 2000; Wu et al., 2005). Although these trends are based on historical observations, similar results were detected following analysis of the Ishii dataset,

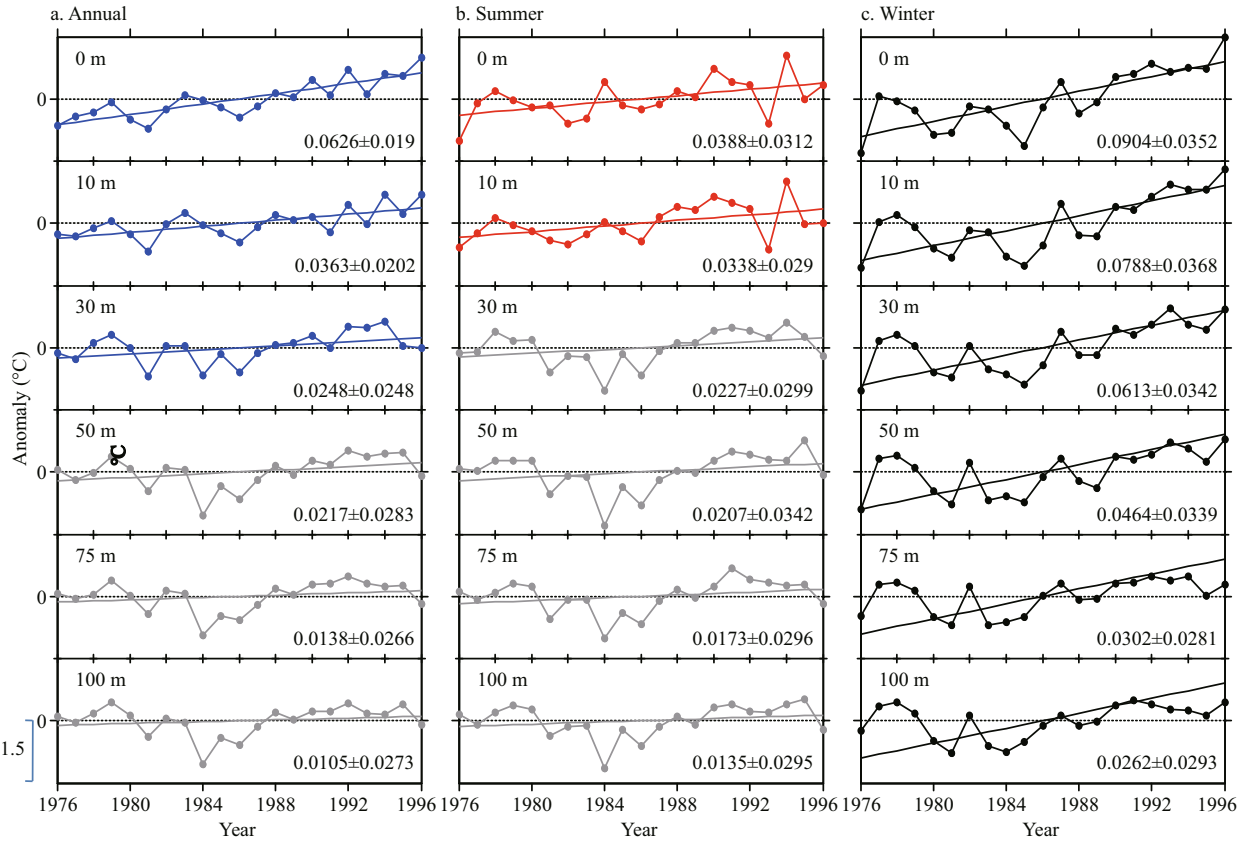

Fig.2 Time series of the ECS upper-ocean temperature anomalies (°C) and associated linear trends (°C/a) during 1976–1996

a. time series (solid lines with filled circles) and associated linear regression lines (bold lines) of the annual mean at the depths of 0, 10, 30, 50, 75, and 100 m (from top to bottom), with corresponding slopes and confidence intervals shown in the bottom-right corner; b and c. as in (a) but for summer and winter, respectively. Blue, red, and black colors in each column highlight the slopes that reach statistical significance above the 90% confidence level using a two-tailed Student *t*-test. Unit length of the graphical scale in the lower left denotes 1.5°C.

highlighting the validity of our results (Supplementary Fig.S1).

3.2 Spatial patterns of annual mean temperature trends

According to the observations, we plotted the spatial patterns of the linear trends in annual mean temperature at the different layers during 1976–1996 (Fig.3). We considered the accumulated temperature increment during the entire period as the trend in each grid to make the results clearer. Over the entire ECS, the SST pattern displays a consistent warming trend (Fig.3a), and the warming is prominent along the paths of the major warm current systems, including the Taiwan Warm Current, Kuroshio Current, Yellow Sea Warm Current (YSWC), and Tsushima Current. The warmest area is located to the north of Taiwan Island (maximum: >5°C within the depth of 30 m), coinciding with the "hot-spot" phenomenon (Wu et al., 2012). Moreover, the warming trend declines gradually with increasing depth, and it becomes confined to the areas of the major warm currents at the deeper layers (Fig.3b–f). It is interesting to note a prominent cooling trend with magnitude >5°C in the southeast of Bohai Bay and the northern Yellow Sea (Fig.3c), which extends to the Changjiang Estuary below the surface, although it also weakens with increasing depth. Other areas of moderate cooling are evident in the southern parts of the Japan/East Sea and to the southeast of the Ryukyu Islands at deeper layers.

3.3 Spatial patterns of seasonal temperature trends

Considering the strong influence of the East Asian monsoon on the ECS, and the resultant seasonal differences between summer and winter in terms of the temperature gradient and amount of solar radiation, it is worthwhile discussing the seasonal spatial patterns of subsurface temperature trends using observational data. Here, we focused on the summer (June–August) and winter (December–February) seasons.

The spatial pattern of summer SST trend demonstrates moderate warming with magnitude no larger than 2°C during 1976–1996 (Fig.4a). The

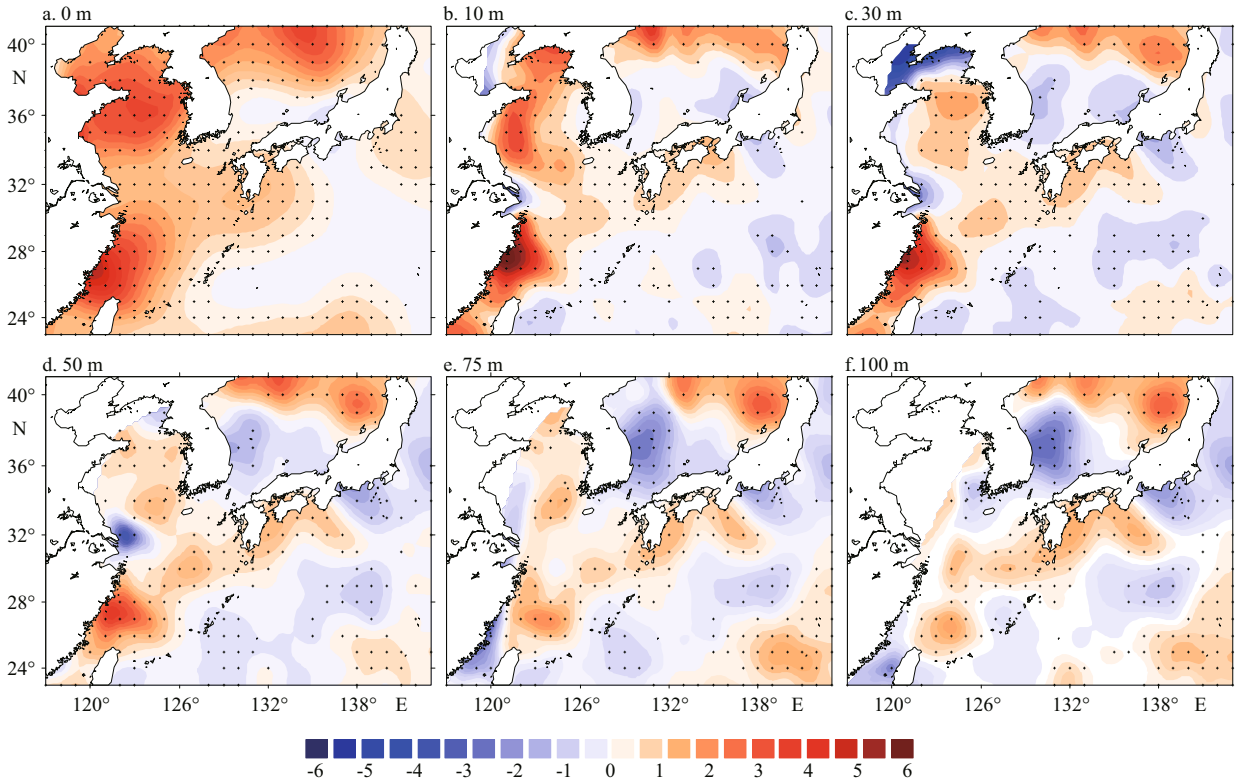

Fig.3 Spatial patterns of linear trends in annual mean upper-ocean temperature

a. spatial pattern of annual mean SST trend during 1976–1996. The accumulated temperature increment (°C) during the entire period is taken as the trend in each grid; b–f. as in (a) but for 10, 30, 50, 75, and 100 m, respectively. Stippling denotes where linear trends are statistically significant above the 90% confidence level.

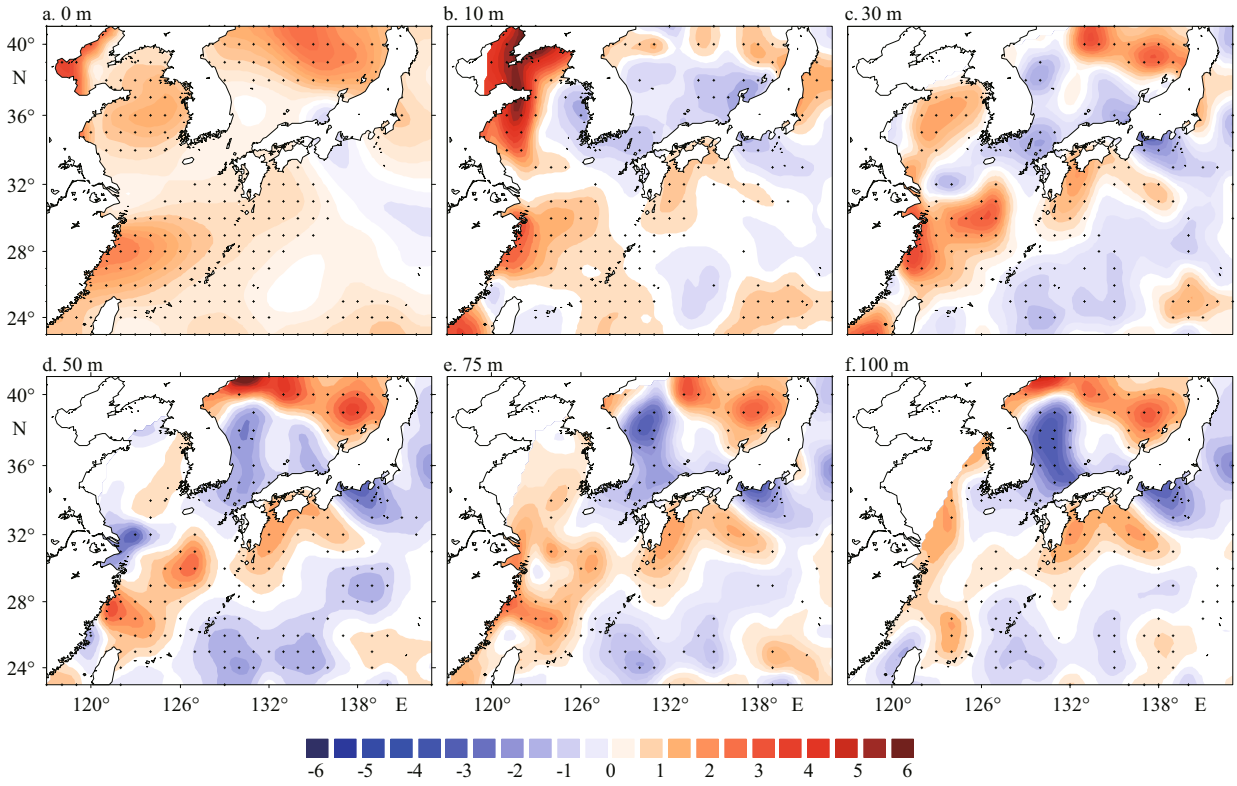

Fig.4 Spatial patterns of linear trends in summer upper-ocean temperature

a. spatial pattern of summer SST trend during 1976–1996. The accumulated temperature increment (°C) during the entire period is taken as the trend in each grid; b–f. as in (a) but for 10, 30, 50, 75, and100 m, respectively. Stippling denotes where linear trends are statistically significant above the 90% confidence level.

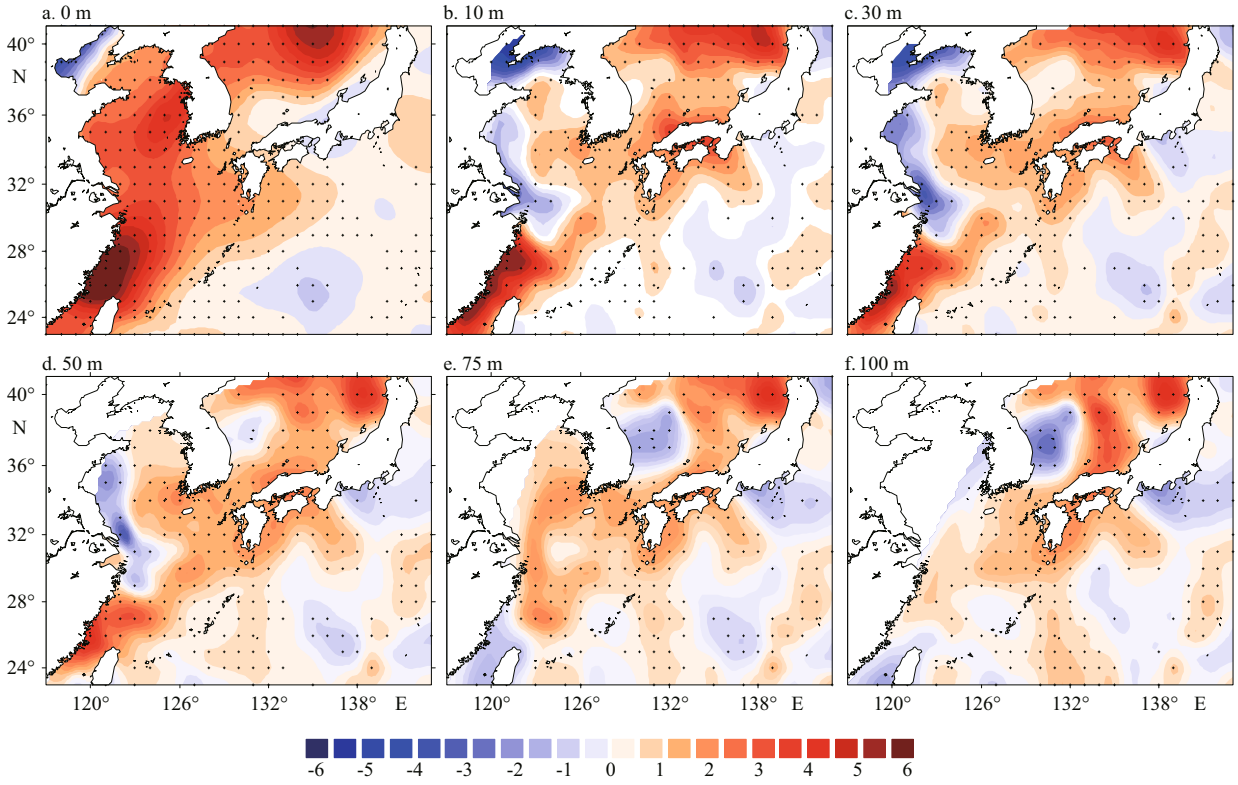

Fig.5 Spatial patterns of linear trends in winter upper-ocean temperature

a. spatial pattern of winter SST trend during 1976–1996. The accumulated temperature increment (°C) during the entire period is taken as the trends in each grid; b–f. as in (a) but for 10, 30, 50, 75, and100 m, respectively. Stippling denotes where linear trends are statistically significant above the 90% confidence level.

warming covers almost the entire region of the ECS. Just below the surface, remarkable warming is evident at the 10-m layer throughout the entire Bohai Sea and in the northwestern Yellow Sea (Fig.4b). The temperature increment in this region exceeds 5°C during the period. This pronounced warming, which is presumed attributable to heating by the atmosphere, reflects the shallow bathymetry (Xie et al., 2002). However, the warming trends decline with depth. In addition to pronounced warming of the shallow coastal waters of China, warming trends are evident along the main warm currents in deeper layers. Areas of cooling are apparent off the coast of China, i.e., southern parts of the Japan Sea and the region to the southeast of the Kuroshio Current.

In winter, the warming trends in the upper ocean are more significant along the warm currents and they extend over wider areas than in summer (Fig.5). In particular, robust "hot spots" are located to the northeast of Taiwan Island, where the Kuroshio Current and the Taiwan Warm Current enter the ECS, and in the northeast of the Japan Sea with warming in the upper layers of >6°C (Fig.5a–c). Although winter warming weakens gradually with increasing depth, it does cover broader areas compared with summer. The Bohai Sea presents cooling trends in winter (Fig.5b, c), opposite to the robust trends of warming detected in summer. Resembling the annual mean pattern, an area of cooling with magnitude no greater than 3°C extends to the Changjiang Estuary and it weakens with increasing depth. In winter, the intensified northward YSWC (Lin et al., 2011) promotes warming along the warm current in the central ECS. To compensate the increased YSWC transport, southward coastal cold currents along the Chinese shelf are reinforced, resulting in cooling of the coastal waters, which is distinctly different from summer.

Comparison of the patterns of annual mean, summer, and winter trends reveals that the annual mean temperature patterns are most similar to those in winter from the perspective of warming/cooling areas and magnitude; thus, winter is dominant in the patterns of upper-ocean temperature variations in the ECS. Moreover, warming/cooling trends are prominent along the paths of warm/cold currents in winter, which is a feature related closely to the dominant role of the circulations in winter. In addition, similar results obtained from analysis of the Ishii dataset validate and support the above conclusions (Supplementary Figs.S2–S4).

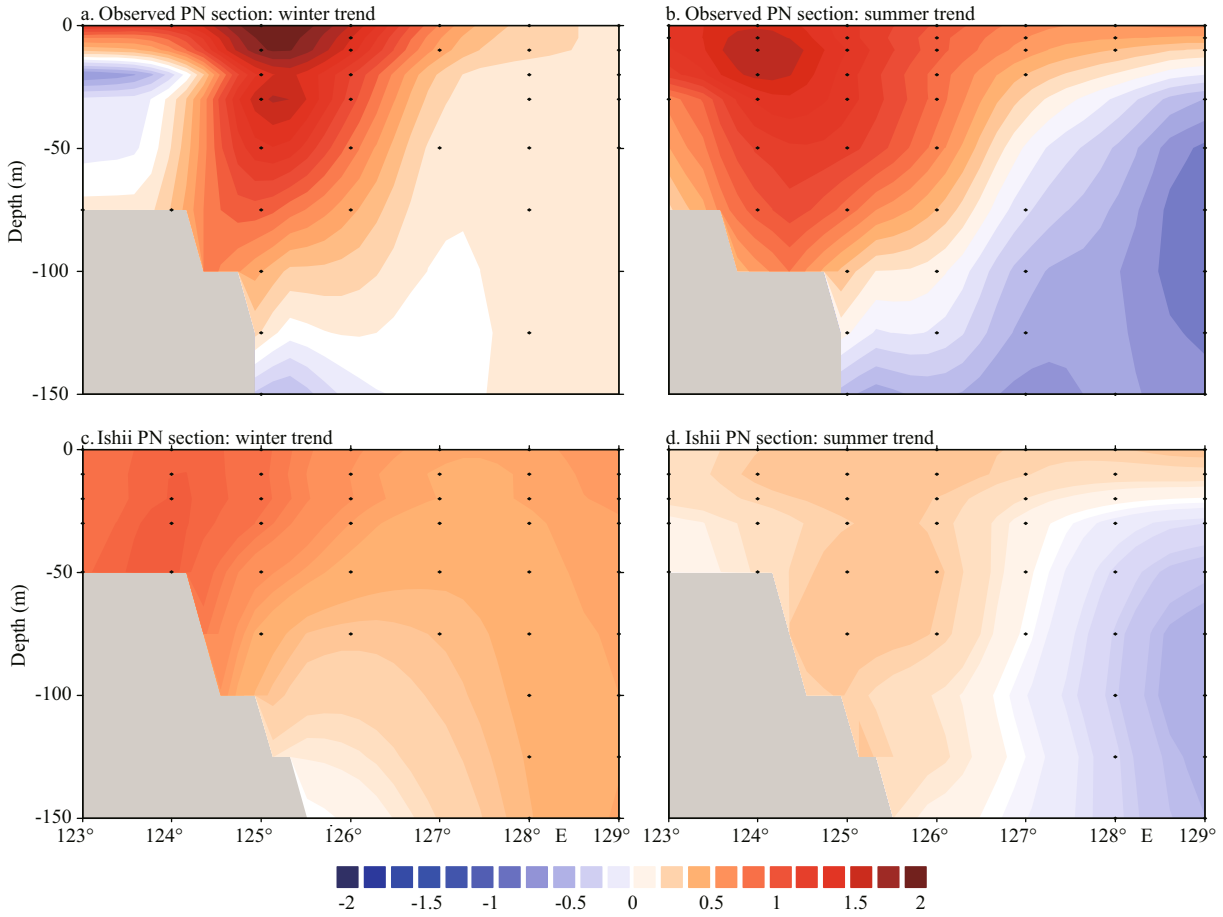

Fig.6 Vertical patterns of temperature trend across the PN section

a. the linear trend (°C) of winter temperature in the vertical profile across the PN section obtained from observational data. Color shading denotes the temperature trend and the gray area denotes the bottom shelf and regions lacking observations; b–d. as in (a) but for summer from the observations, and for winter and summer from the Ishii dataset, respectively. Stippling denotes where linear trends are statistically significant above the 90% confidence level.

3.4 Temperature trends in routine sections

As the upper-ocean winter warming trends in the ECS are confined mainly to the areas of the major warm currents, and because winter accounts for the largest part of the annual mean trends, we examined the temperature trends of the two routine sections (PN and 34°N) based on observations that are more reliable and uniform in distribution.

The Kuroshio Current is a robust western boundary current of the North Pacific subtropical gyre. It transports huge amounts of nutrients and heat poleward and it exerts important dynamic and thermal effects on the ECS (Guan, 1988). It enters the ECS to the east of Taiwan Island and it exits from the area to the south of the island of Yakushima, Japan (30.5°N, 130.5°E). The Kuroshio Current crosses the PN section in the central ECS (Fig.1, red bold line). The hydrographic data along this section are sufficiently dense that the vertical structure of the temperature variation of the Kuroshio axis can be detected. We constructed seasonal temperature linear trends of the PN section for the period 1976–1996. Trends for winter and summer derived from the hydrographic observations are shown in the upper panels of Fig.6 and those based on analysis of the Ishii dataset are shown in the lower panels. The observational data show robust warming along the PN section at 124.5°–125.5°E in winter with magnitude >2°C (Fig.6a), and at 123.5°–124.0°E in summer with magnitude no greater than 1.5°C (Fig.6b). These significant warming trends generally cross the main stream of the Kuroshio Current and extend to the depth of 125 m. In addition to the stream of the Kuroshio Current, moderate warming occurs over most of the remainder of the entire profile in winter, whereas some cooling areas appear in summer.

In summary, the vertical structure of temperature variation is consistent with the structure of the core of the Kuroshio Current (Wei et al., 2013); i.e., the warming is restricted to the current stream, and it is more robust in winter than in summer. Furthermore,

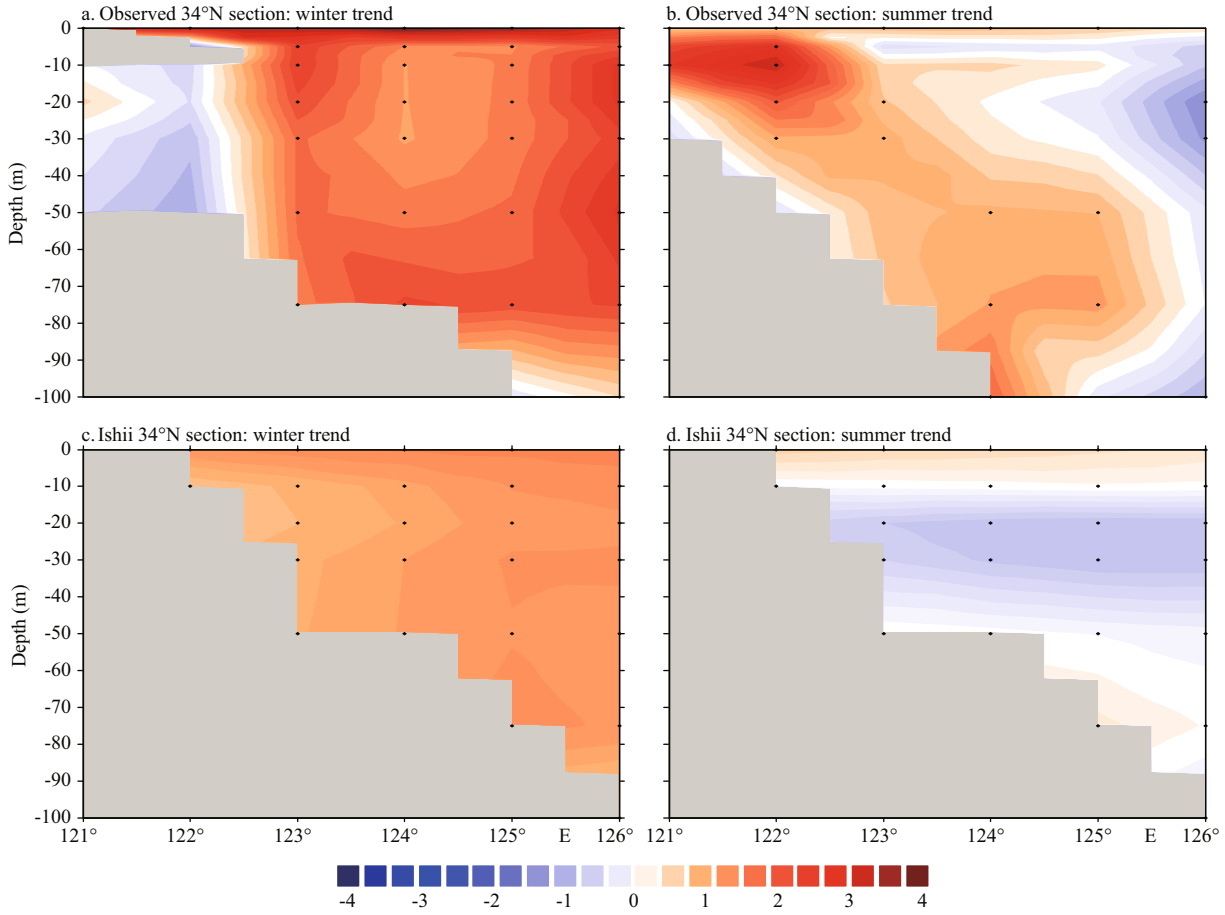

Fig.7 Vertical patterns of temperature trend across the 34°N section

a. the linear trend (°C) of winter temperature in the vertical profile across the 34°N section obtained from observational data. Color shading denotes the temperature trend and gray areas denote the bottom shelf and regions lacking observations; b–d. as in (a) but for summer from the observations, and for winter and summer from the Ishii dataset, respectively. Stippling denotes where linear trends are statistically significant above the 90% confidence level.

since the 1980s, an increase in heat advection across the PN section via the Kuroshio Current has been observed by the Japan Meteorological Agency (Weng et al., 1996). This might support the view that horizontal heat advection accelerates the rapid warming of the ECS (Feng and Lin, 2009; Zhang et al., 2010).

The existence of the YSWC is presented based on observations of earlier studies (Lin et al., 2011; Lin and Yang, 2011) and the mechanism of its westward shift is analyzed. It is elucidated that the YSWC originates from the Kuroshio Current, and that variations in the Taiwan Warm Current, Kuroshio Current, and Tsushima Warm Current inevitably influence the YSWC (Xu et al., 2009). Given that the main axis of the YSWC crosses the routine 34°N section (Fig.1; red bold line), the vertical structure of the temperature trends in this section depict the variations along the axis of the YSWC. The warming trend along the 34°N section in winter is strong in most parts of the profile, and the warm axis is located at about 123°E with a warming trend >2°C, which coincides with the high-temperature core of the YSWC (Lin et al., 2011). In addition, cooling trends are detected west of 122°E below the surface, which are related to the southward coastal cold currents along the Chinese shelf. In summer, a notable warm core lies at around 122°E in the upper layers, which corresponds to the remarkable warming of the nearshore shallow waters, and it declines gradually with increasing depth. Furthermore, some areas of cooling are located to the east of 125°E.

According to the trends along the routine PN and 34°N sections, the warming/cooling trends in winter are confined mainly to the realms of the warm/cold currents, implying a dominant role of horizontal advection in relation to the temperature variations. However, warming in summer is forced primarily by the atmosphere and the effect of oceanic circulation plays a secondary role. In addition, analysis of the Ishii dataset illustrates similar yet relatively weaker warming trends (Fig.7c, d) that support our observational results.

4 CONCLUSION

This study investigated the regional mean and spatial patterns of upper-ocean sea temperature trends in the ECS during the period of rapid warming (1976–1996) based on hydrographic observational data.

Over the entire ECS, significant warming trends were identified following a regime shift in 1976, and the warming trends in winter were found to be of greater magnitude and to extend across wider areas than in summer. In other words, the prominent "hot spot" identified in earlier studies was found to occur mainly in winter. Although the magnitudes of the trends in winter were found to weaken gradually with increasing depth, the warming was concentrated along the major warm currents, highlighting the leading role of horizontal advection in winter. It was found that the warming in summer was influenced primarily by both the atmosphere and the bathymetry. Furthermore, the spatial patterns of the annual mean trends were shown to resemble those of winter from the perspective of the locations of the areas of warming/cooling and their magnitudes, reflecting the dominance of winter on the pattern of temperature variations. In addition, the vertical structures of the temperature trends of the routine PN and 34°N sections confirmed that warming in winter is attributable mainly to the circulation.

Analysis of the Ishii dataset revealed similar but relatively weaker warming trends as found from the observational data, validating and supporting our findings. However, analysis of the Ishii dataset failed to capture either the prominent "hot spot" to the north of Taiwan Island or the cold core in Bohai Bay. The difference between the two datasets could perhaps be attributed to the analysis technique or to the methods of incorporation and smoothing of the analyzed data. Thus, the observational data could be better for reliable and sensitive interpretation of the oceanic processes in the ECS.

The preliminary results of this study suggest that horizontal advection plays a dominant role in temperature variation within the ECS in winter, whereas atmospheric forcing and bathymetry are important in summer. However, it is recognized that temperature variations within the ECS are also influenced by other factors, e.g., the mixed-layer depth and vertical entrainment; thus, the effects of these and other factors will be investigated in future research.

5 DATA AVAILABILITY STATEMENT

The hydrographic observational data analyzed in the current study are not publicly available because they contain information that could compromise research participant privacy; however, they are available from the corresponding author upon reasonable request. The analyzed data that support the findings of this study are available as Subsurface Temperature and Salinity Analyses by Ishii et al. at the National Center for Atmospheric Research, Computational and Information Systems Laboratory (http://rda.ucar.edu/datasets/ds285.3/).

6 ACKNOWLEDGEMENT

We thank the Frontier Research System for Global Change, Japan Marine Science and Technology Center for providing data. We also thank the two anonymous reviewers for providing useful suggestions that helped greatly with improving the quality of the manuscript.

References

Cai R S, Chen J L, Huang R H. 2006. The response of marine environment in the offshore area of China and its adjacent ocean to recent global climate change. *Chinese Journal of Atmospheric Sciences*, **30**(5): 1 019-1 033. (in Chinese with English abstract)

Chen X R, Cai Y, Tan J, Huang Y Y, Wang L. 2014. Research progress on hiatus in the process of global warming. *Advances in Earth Science*, **29**(8): 947-955. (in Chinese with English abstract)

Chen Y L, Ho C R. 2002. A study on global and regional sea surface temperature trends. *Journal of Photogrammetry and Remote Sensing*, **7**: 41-58.

Conkright M E, Antonov J I, Baranova O K, Boyer T P, Garcia H E, Gelfeld R, Johnson D, Locarnini R A, Murphy P P, O'Brien T D, Smolyar I, Stephens C. 2002. World ocean database 2001, Vol. 1: introduction. *In*: Levitus S ed. NOAA Atlas NESDIS 42. U.S. Government Printing Office, Washington, DC. 167p.

Cressman G P. 1959. An operational objective analysis system. *Mon. Wea. Rev*, **87**(10): 367-374.

Easterling D R, Wehner M F. 2009. Is the climate warming or cooling? *Geophysical Research Letters*, **36**(8): L08706, https://doi.org/10.1029/2009GL037810.

Feng L, Lin X P. 2009. Long-term trend of the East China Sea surface temperature during 1945~2006. *Periodical of Ocean University of China*, **39**(1): 13-18. (in Chinese with English abstract)

Guan B X. 1988. Major features and variability of the Kuroshio in the East China Sea. *Chinese Journal of Oceanology and Limnology*, **6**(1): 35-48.

Ishii M, Kimoto M, Kachi M. 2003. Historical ocean subsurface

temperature analysis with error estimates. *Monthly Weather Review*, **131**(1): 51-73.

Ishii M, Kimoto M, Sakamoto K, Iwasaki S I. 2006. Steric sea level changes estimated from historical ocean subsurface temperature and salinity analyses. *Journal of Oceanography*, **62**(2): 155-170.

Latif M, Barnett T P. 1994. Causes of decadal climate variability over the North Pacific and North America. *Science*, **266**(5185): 634-638.

Levitus S, Boyer T P, Antonov J. 1994. World Ocean Atlas 1994, Vol. 5: Interannual Variability of Upper Ocean Thermal Structure. NOAA Atlas NESDIS, Maryland, USA. 176p.

Lin C L, Su J L, Xu B R, Tang Q S. 2001. Long-term variations of temperature and salinity of the Bohai Sea and their influence on its ecosystem. *Progress in Oceanography*, **49**(1-4): 7-19, https://doi.org/10.1016/s0079-6611(01)00013-1.

Lin C, Ning X, Su J, Lin Y, Xu B. 2005. Environmental changes and the responses of the ecosystems of the Yellow Sea during 1976-2000. *Journal of Marine Systems*, **55**(3-4): 223-234, https://doi.org/10.1016/j.jmarsys.2004.08.001.

Lin X P, Xu L X, Li J P, Luo D H, Liu H L. 2016. Research on the global warming hiatus. *Advances in Earth Science*, **31**(10): 995-1 000, https://doi.org/10.11867/j.issn.1001-8166.2016.10.0995. (in Chinese with English abstract)

Lin X P, Yang J Y, Guo J S, Zhang Z X, Yin Y Q, Song X Z, Zhang X H. 2011. An asymmetric upwind flow, Yellow Sea Warm Current: 1. New observations in the western Yellow Sea. *Journal of Geophysical Research*: *Oceans*, **116**(C4): C04026, https://doi.org/10.1029/2010jc006513.

Lin X P, Yang J Y. 2011. An asymmetric upwind flow, Yellow Sea Warm Current: 2. Arrested topographic waves in response to the northwesterly wind. *Journal of Geophysical Research*: *Oceans*, **116**(C4): C04027, https://doi.org/10.1029/2010jc006514.

Liu Q Y, Xie S P, Li L J, Maximenko N A. 2005. Ocean thermal advective effect on the annual range of sea surface temperature. *Geophysical Research Letters*, **32**(24): L24604, https://doi.org/10.1029/2005GL024493.

Liu Q Y, Zhang Q. 2013. Analysis on long-term change of sea surface temperature in the China Seas. *Journal of Ocean University of China*, **12**(2): 295-300, https://doi.org/10.1007/s11802-013-2172-2.

Park W S, Oh I S. 2000. Interannual and interdecadal variations of sea surface temperature in the East Asian Marginal Seas. *Progress in Oceanography*, **47**(2-4): 191-204.

Smith N R. 1995. An improved system for tropical ocean subsurface temperature analyses. *Journal of Atmospheric and Oceanic Technology*, **12**(4): 850-870.

Tang X H, Wang F, Chen Y L, Li M K. 2009. Warming trend in northern East China Sea in recent four decades. *Chinese Journal of Oceanology and Limnology*, **27**(2): 185-191, https://doi.org/10.1007/s00343-009-9238-4.

Tian Y J, Akamine T, Suda M. 2003. Variations in the abundance of Pacific saury (*Cololabis saira*) from the northwestern Pacific in relation to oceanic-climate changes. *Fisheries Research*, **60**(2-3): 439-454.

Tomita T, Xie S P, Nonaka M. 2002. Estimates of surface and subsurface forcing for decadal sea surface temperature variability in the mid-latitude North Pacific. *Journal of the Meteorological Society of Japan Series II*, **80**(5): 1 289-1 300.

Wang F, Meng Q J, Tang X H, Hu D X. 2013. The long-term variability of sea surface temperature in the seas east of China in the past 40 a. *Acta Oceanologica Sinica*, **32**(3): 48-53, https://doi.org/10.1007/s13131-013-0288-2.

Wei Y Z, Huang D J, Zhu X H. 2013. Interannual to decadal variability of the Kuroshio Current in the East China Sea from 1955 to 2010 as indicated by in-situ hydrographic data. *Journal of Oceanography*, **69**(5): 571-589, https://doi.org/10.1007/s10872-013-0193-5.

Weng X C, Zhang Q L, Yang Y L, Yan T Z. 1996. The Kuroshio heat transport in the East China Sea and its relation to the precipitation in the rainy season in the Huanghuai Plain area. *Oceanologia et Limnologia Sinica*, **27**(3): 237-245. (in Chinese with English abstract)

White W B. 1995. Design of a global observing system for gyre-scale upper ocean temperature variability. *Progress in Oceanography*, **36**(3): 169-217, https://doi.org/10.1016/0079-6611(95)00017-8.

Wu D X, Li Q, Lin X P, Bao X W. 2005. The characteristics of the Bohai Sea SST anomaly interannual variability during 1990~1999. *Periodical of Ocean University of China*, **35**(2): 173-176. (in Chinese with English abstract)

Wu L X, Cai W J, Zhang L P, Nakamura H, Timmermann A, Joyce T, McPhaden M J, Alexander M, Qiu B, Visbeck M, Chang P, Giese B. 2012. Enhanced warming over the global subtropical western boundary currents. *Nature Climate Change*, **2**(3): 161-166, https://doi.org/10.1038/nclimate1353.

Xie S P, Hafner J, Tanimoto Y, Liu W T, Tokinaga H, Xu H M. 2002. Bathymetric effect on the winter sea surface temperature and climate of the Yellow and East China Seas. *Geophysical Research Letters*, **29**(24): 2228, https://doi.org/10.1029/2002gl015884.

Xu L L, Wu D X, Lin X P, Ma C. 2009. The study of the Yellow Sea Warm Current and its seasonal variability. *Journal of Hydrodynamics*, *Ser*. *B*, **21**(2): 159-165.

Zhang L P, Wu L X, Lin X P, Wu D X. 2010. Modes and mechanisms of sea surface temperature low-frequency variations over the coastal China seas. *Journal of Geophysical Research*: *Oceans*, **115**(C8): C08031, https://doi.org/10.1029/2009jc006025.

Zhang X Z, Qiu Y F, Wu X Y. 2005. The long-term change for sea surface temperature in the last 100 years in the offshore sea of China. *Climatic and Environmental Research*, **10**(4): 799-807.

Electronic supplementary material

Supplementary material (Supplementary Figs.S1–S4) is available in the online version of this article at https://doi.org/10.1007/s00343-019-7278-y.